Experimental and Computational Multiphase Flow
Vol. 3, No. 4, 2021, 242–249
https://doi.org/10.1007/s42757-020-0071-5

Simulation of water evaporation under natural conditions—A state-of-the-art overview

Daniel Wickert (✉), Günther Prokop

Technische Universität Dresden, Dresden, 01069, Germany

Abstract

The phase change of water or other liquids is a process that takes part in many technical applications. The field of research is widely diversified with domains in energy technology, air conditioning, and even corrosion. The modalities of the phase change vary thereby. While condensation always occurs under the same condition, evaporation is much more complicated. The evaporation of a liquid can be forced by boiling or happens under natural condition. Boiling is a process with a high-energy flow and therefore a fast procedure. Evaporation under natural conditions is a much more time-intensive process but in researches of the wetting and as a result the damage of daily products more relevant. This contribution analyses different CFD-tools with regard to their ability to simulate the evaporation of water under natural conditions and gives an overview of the state-of-the-art for a few mesh and meshfree methods. The mesh-based CFD showed varying results from unsuitable models to detailed calculations. The mesh-free CFD is dependent on an artificial model due to some methodological assumptions. As a conclusion, the use of an artificial model is recommended in order to be able to generate a usable result and evaluate the benefit of countermeasures.

Keywords

SPH
phase change
VOF
evaporation

Article History

Received: 13 February 2020
Revised: 7 April 2020
Accepted: 16 April 2020

Research Article

1 Introduction

Fluid flows are a very complex process that is increasingly coming into focus, motivated by ongoing optimizations of products and workflows or just by researches to gain a better understanding of specific events (Hermsdorf et al., 2016). A CFD analysis is often more economic than the corresponding experiment due to the analysis of a not yet existing prototype and even allows the research of difficult-to-examine processes, e.g., of highly aggressive fluids. Modern CFD-solutions make it easy to handle a wide variety of problems and the rising computation power of workstations leads to less computation time. In this context, the CFD-model either gets adapted for a more accurate resolution or receives new computation models to simulate problems that are more complex, e.g., moving boundaries or free surface flows. Depending on the simulated problem and the needed accuracy exists a software solution that can calculate the problem in minutes on a workstation up to a couple of days on a cluster. This paper is an extract of the development of a new method, which focuses on the phase change of water as part of the determination of the wetting state of components in a machine, e.g., an automobile (Jahn and Prokop, 2016). For this, the state-of-the-art of a few software solutions of the conventional CFD and the meshfree SPH-method are analyzed and compared to experimental data.

The paper starts with a short introduction to the different CFD methods with regard to the discretization of the simulated area, goes on with the evaporation process, and presents the experiment for the benchmark before analyzing and comparing the different software solutions.

2 Theory

2.1 CFD

The CFD is an abbreviation for computational fluid dynamics and describes a tool to analyze flows with numerical models. These models are based on the conservation laws for energy, mass and momentum, and others in the form of a partial differential equation (Ferziger and Peric, 2008; Schwarze, 2013). In general, the software delivers an approximate solution, which is caused by the usage of models, justified by a non-existing exact solution or the unacceptable

✉ Daniel.Wickert@tu-dresden.de

Nomenclature

A	Function	u_x	Velocity component in x-direction
E	Total energy	V	Volume
g	Gravity	W	Kernel function
h	Smoothing length	x_x	Position of element x
m	Mass	α_i	Volume fraction of phase i
p	Pressure	δ	Kronecker function
q_x	Conductive heat flux in x-direction	ρ_x	Density of phase x
S	Source term		

computation time for this. The quality of the solution depends thereby on the discretization (Ferziger and Peric, 2008). The most common approaches are the Finite-Volume-, the Finite-Difference-, and the Finite-Elements-Method. There are numerous additional approaches but their application are often limited to specific scenarios.

There are also multiple approaches to simulate multiphase flows, depending on the detail and the flow characteristics. For the explicit tracking of free surfaces, the Volume-Of-Fluid (VOF) method is often recommended. This approach uses the following equations for the conservation laws (Hirt and Nichols, 1981; Alizadehdakhel et al., 2010):

Continuity:

$$\frac{\partial}{\partial t}(\rho)+\sum_{j=1}^{3}\frac{\partial}{\partial x_i}(\rho u_j)=S_{\mathrm{M}}$$

Momentum:

$$\frac{\partial}{\partial t}(\rho u_i)+\sum_{j=1}^{3}\frac{\partial}{\partial x_i}(\rho u_i u_j)=-\frac{\partial p}{\partial x_i}+\sum_{j=1}^{3}\frac{\partial}{\partial x_i}\left[\mu\left(\frac{\partial u_i}{\partial x_j}+\frac{\partial u_j}{\partial x_i}-\frac{2}{3}\delta_{ij}\sum_{i=1}^{3}\frac{\partial u_i}{\partial x_i}\right)\right]+S_{\mathrm{F},i}$$

Energy:

$$\frac{\partial}{\partial t}(\rho E)+\sum_{j=1}^{3}\frac{\partial}{\partial x_j}(\rho E u_j)=\sum_{i=1}^{3}\sum_{j=1}^{3}\left(\frac{\partial}{\partial x_j}(\tau_{ij})u_i\right)-\sum_{j=1}^{3}\frac{\partial}{\partial x_j}q_j+S_{\mathrm{E}}$$

The interface between the phases is tracked by the volume fraction (Siemens, 2019):

$$\alpha_i=\frac{V_i}{V}$$

The volume fraction of each cell must sum up to one.

The conventional CFD needs a mesh to calculate the properties of the flow. This mesh forms the area of the simulation area with a finite number of points, which are connected to each other (Liu and Liu, 2010) (Fig. 1).

By often using an iterative process, the software solves the differential equations to calculate the physical properties of the flow. The quality of the result thereby depends on the resolution of the mesh (Ferziger and Peric, 2008). A complex geometry or the exact solution of a complex flow can lead to a very fine mesh with a high number of cells, which leads to high computation time. In addition to that is the tracking of moving objects or deformable boundaries still a formidable task (Liu and Liu, 2010). Table 1 lists a few characteristic properties of the VOF-method for simulating multiphase flows.

The opposite of this are methods, which do not depend on a mesh, e.g., the Smoothed-Particle-Hydronamics (SPH) method as it is used in this paper and hybrids of both methods. The discretization in this method also takes place by dividing and representing the simulated area with a high number of data points for the fluid and objects (particles), which are comparable to the nodes in a mesh, but not connected to each other in this case. In contrast to the

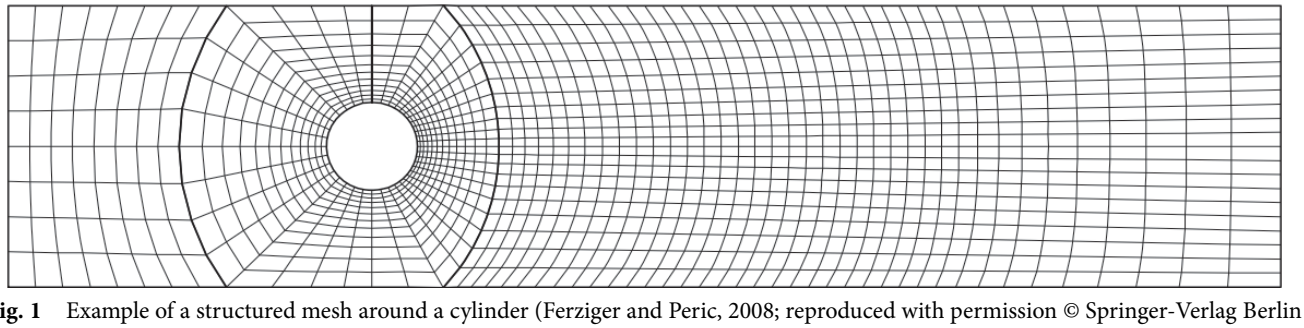

Fig. 1 Example of a structured mesh around a cylinder (Ferziger and Peric, 2008; reproduced with permission © Springer-Verlag Berlin Heidelberg 2008).

Table 1 Characteristic properties of the VOF-method (Liu and Liu, 2010; Sun and Tao, 2010; Ihmsen, 2013)

Advantage	Disadvantage
Conservation of mass is granted	Difficult to calculate accurate local curvature
Sharp representation of the interface	High resolution and small time-step necessary
	Discretization of the complete simulated area

Table 2 Characteristic properties of the SPH method (Liu and Liu, 2010; Wickert et al., 2020)

Advantage	Disadvantage
Numerical quality independent of a mesh	Not as developed as meshbased methods
No explicit interface tracking for multiphase flows	Can deliver unphysical results
	Spatial derivatives computationally expensive

Euler-approach of the meshbased CFD uses the particle-method a Lagrange approach in which the neighbor particle is not fixed. This leads to a different mathematical system (Becker and Teschner, 2007):

Continuity:

$$\frac{\partial \rho_i}{\partial t} = \sum_j m_j u_{ij} \nabla_i W_{ij}$$

Momentum:

$$\frac{\partial u_i}{\partial t} = -\sum_j m_j \left(\frac{p_i}{\rho_i^2} + \frac{p_j}{\rho_j^2} \right) \nabla_i W_{ij} + g$$

Each particle represents a small finite volume of the area (Monaghan, 1992; Liu and Liu, 2010; Ihmsen, 2013). The physical condition of each particle is calculated by an interpolation of its neighbored particles and limited by a weighting function (Fig. 2):

$$A(x_i) = \sum_j m_j \frac{A_j}{\rho_j} W(x_i - x_j, h)$$

In reliance to the simulated problem, the meshfree methods can have a few advantages despite a simpler discretization of complex objects and flows (Liu and Liu, 2010) (Table 2). In general, the application of the meshfree methods is often only suitable for a specific field of application.

2.2 Evaporation

The fundament of this paper is the simulation of evaporation

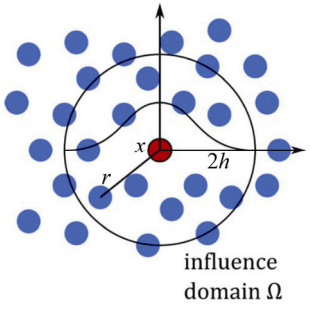

Fig. 2 Influence domain in SPH (Sun et al., 2013; reproduced with permission © Elsevier Inc. 2013).

of a liquid using CFD. Until today, this is still a challenge for the CFD-tools. To improve the understanding of the tool-analysis later, this chapter describes the process of the phase change of water with the help of the Mollier-diagram. The evaporative process has to be differed between performing at the saturation temperature or below (Kraume, 2012). In both cases, the water changes its state of aggregation but at the saturation temperature, in the following labeled as vaporization, boiling can occur and needs a different mathematical description from evaporation below the saturation temperature under natural conditions. Another difference is the composition of the surrounding gas phase. While the surrounding gas phase during the evaporation contains at least one more species than steam, the gas phase during vaporization consists only of steam (Kraume, 2012). Since these processes consist of multiple coupled complex models, a generally valid mathematical model does not exist yet.

In the following is only an explanation of the evaporation process with water and air, since vaporization is not relevant for this paper. The surrounding air has a specific state of temperature and humidity, defined as state 1 in Fig. 3 and delivers the necessary energy for the process while it flows across the water surface (Kraume, 2012). A second air layer right above the water surface (state 2 in Fig. 3) is fully saturated with steam. While the air of state 1 flows across the water surface, it comes to a mixture process with the air layer of state 2 and a new condition of the air (state 3) is the result. This air mass absorbs again steam until it is saturated and the process starts again (Skolaut, 2018). At the same time, the crossing air mass lowers its temperature due to the energy transfer of the evaporation and the humidity rises. The energy transfer rises the water temperature slightly while the evaporation process lowers it. This process can be continued until a stationary condition is reached, either by reaching the saturation point of the air or by reaching the steady-state temperature as a result of the possible heat transfer (Kraume, 2012).

3 Experiment

The analysis starts with the experiment in order to get the right boundary conditions. As already mentioned is this

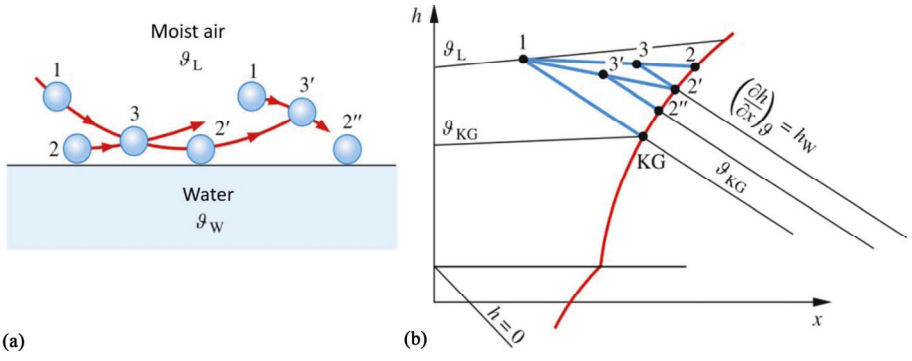

Fig. 3 Evaporation process schematic (a) and in the Mollier-diagram (b) (Skolaut, 2018; reproduced with permission © Springer-Verlag GmbH Deutschland, ein Teil von Springer Nature 2018).

paper part of the virtual determination of the wetting state of components in a machine. In this consequence, a small amount of water shall evaporate under natural conditions. For this, 20 mL of water is filled in a petri dish with an inner diameter of 90 mm to obtain a large and constant surface size while evaporating. During the evaporation process, the petri dish is placed in a room with nearly constant conditions of 35 °C and 32 %rH, measured with a DKRF400 probe. The probe has an accuracy of ±0.4 °C as well as ±1.8 %rH in the needed measuring range. To reduce the airflow, only one wall has two small openings for ventilation all others are closed (Fig. 4). The existing airflow, measured with a thermal anemometer of type testo 405i, is less than 0.01 m/s. This is below the accuracy ±0.1 m/s of the probe. Under these circumstances, the assumption is made that the mass transport takes place by natural convection. A precision scale of type Lutron GM-500 with a resolution of 0.1 g measures the reduction of the water mass during the experiment. An additional control volume with a class 1 Type K thermocouple measures the water temperature at certain time marks to reduce its influence on the evaporation process. The evaporation of the water is below the minimum weight of the scale after 31 h and takes 36 h for the full amount of water according to image evaluation.

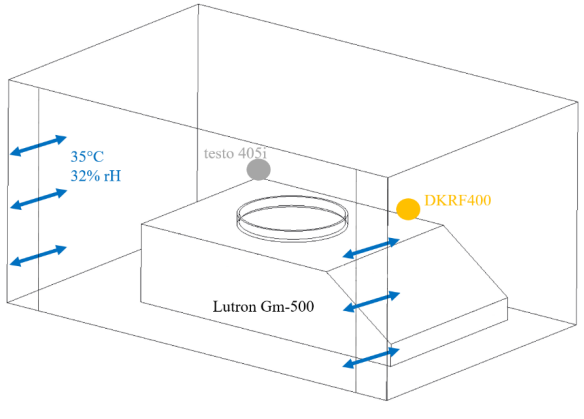

Fig. 4 Schematic representation of the experimental setup.

4 Simulation

The following chapter contains an analysis of a few more or less common software solutions. Each analysis starts with a closed petri dish, which is expanded to a model from the experiment, if successful. The focus lays on the capability to simulate the scenario from the experiment and how the software computes the process according to the physical accuracy. This always happens with the regard to the application to more complex and varying geometries as it can occur during the development process of new machines. For this application, it is necessary to track the water surface and volume as well as the wetted surfaces. All simulations are done on a workstation with a 6-core Intel I7-4930K and 64 GB RAM.

4.1 Comsol

The first software is Comsol in Version 5.3. Comsol uses the FEM-method to calculate the condition of the flow. To get used to the program, many example simulations are available. Inter alia, a simulation named "Modeling Evaporative Cooling", which is already close to the experiment above and therefore the base for the analysis (Comsol, 2019). In this example, a water glass, filled with hot water, is placed in an airflow and the simulation computes the evaporative cooling of the water in parallel to the mass and heat transfer (Fig. 5). Therefore, the model consists of the three domains air, water glass, and water. The workstation needs less than one hour to calculate the preset 20 min and the achieved results are plausible (Comsol, 2019). Nonetheless, no own simulation model of the experiment was built up because of a few problems. The first is the used equation to calculate the evaporation flux:

$$\dot{m}_{\mathrm{evap}} = K\left(c_{\mathrm{sat}} - c_{\mathrm{v}}\right)M_{\mathrm{v}}$$

with the evaporation rate K, the molar mass of water vapor M_{v} and the vapor (c_{v}), and saturation concentration (c_{sat}) (Comsol, 2019). The evaporation rate K is an artificial

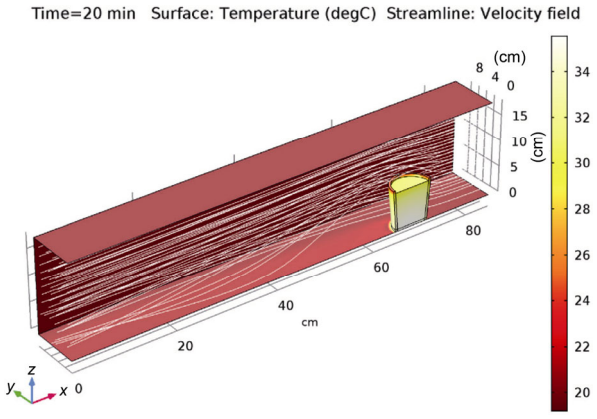

Fig. 5 Result of the Comsol model after 20 simulated minutes (Comsol, 2019)

number, defined by the user. This allows the exact calibration to match experimental data. In this context, the model should be able to simulate similar geometries correctly but the transferability to other, more diverging and complex geometries from the original is questionable.

The second problem is the level of the water. The example has a constant level. To simulate a decreasing level Comsol supports a moving mesh. This leads to higher computation time and the movement of the water level has to be predefined mathematically in each direction. As long as a simple geometry is used, this is not a problem but with regard to simulate the evaporation of water in a more complex geometry, this is not efficiently applicable.

4.2 Ansys Fluent

The next software, as a representative of the FVM-method, is Ansys Fluent in the version 16.2. The analysis starts with the closed petri dish. This defined scenario describes with water and air two immiscible phases with the necessary tracking of a free surface and a phase change; therefore, the VOF-method goes into operation. The complete setup is listed in Table 3.

To model the phase change, Fluent has got an evaporation–condensation model, based on the Lee-model, implemented (ANSYS Inc., 2013). Using a different algorithm is possible by implementing one via a user-defined function but this is not part of this software analysis. In a first attempt, the wall of the closed petri dish is directly heated according to the ambient temperature from the experiment. Since no evaporation could be detected the wall temperature was increased to 393 K to force a faster phase change. The water in the heated area directly starts to boil and vapor bubble rise. After lowering the temperature of the heated area to 372 K, which is just one Kelvin below the boiling point, no phase change occurs, while already a strong vapor stream develops in reality. The missing phase change in Fluent below the boiling point of a fluid is the result of the used Lee-model to calculate the mass transfer.

Table 3 Settings in Ansys Fluent

Parameter	Numerical method
Method	VOF
Time	Transient
Phases	Water (liquid (primary) and vapor); air
Mass transfer	Water to vapor (evaporation–condensation model)
Viscosity	k–ε

$$\dot{m}_{\text{evap}} = coeff * \alpha_{\text{l}} \rho_{\text{l}} \frac{(T_{\text{l}} - T_{\text{sat}})}{T_{\text{sat}}}$$

$$\dot{m}_{\text{cond}} = coeff * \alpha_{\text{v}} \rho_{\text{v}} \frac{(T_{\text{sat}} - T_{\text{v}})}{T_{\text{sat}}}$$

The mass transfer of the evaporation, as well as the condensation, needs the phase fraction α, the density ρ, the temperature and saturation temperature of the fluid or steam in order for calculation. The *coeff* is a user-defined calibration coefficient to match the phase change rate to experimental data (ANSYS Inc., 2013; Sun et al., 2014). The formula shows that the implemented model needs a liquid temperature above its saturation temperature in order to get a positive value and therefore an evaporative mass transfer. In contrast, condensation is only below the saturation temperature computable. In addition to that, the calibration coefficient makes the transferability to other, more diverging geometries questionable as already mentioned at Comsol. The implemented phase change model may fit to certain applications but with regard to the intended application for natural evaporation, Ansys Fluent does not have a fitting model for the VOF-method. Other approaches offer further calculation models such as the thermal phase change from the Eulerian multiphase model. With this model, a representation of the phase change process, similar to Star-CCM+ below the saturation temperature, is probably possible. Since a comparable approach is analyzed with Star-CCM+, no further model of the experiment was developed.

4.3 Star-CCM+

The last mesh-based CFD software is Star-CCM+ in version 14.04. Star-CCM+ also uses the FVM-method and due to the free surface problem the VOF-method is used again. The complete setup is listed in Table 4.

Star-CCM+ was able to simulate the closed petri dish. Based on this, the model of the experiment followed, whose special features are described in the following. To track the decreasing water level properly the inside of the petri dish needs a much smaller cell size than the surrounding area of the room, which leads to a total cell number of 125,000. Because of the missing airflow, the model consists of two

Table 4 Settings in Star-CCM+

Parameter	Numerical method
Method	Eulerian multiphase → VOF
Time	Transient
Phases	Multi-component → water, air + water
Mass transfer	Evaporation–condensation model/VOF–VOF interaction
Viscosity	k–ε

outflows, which allow a backflow with room conditions. At the initialization, the air temperature, the liquid temperature and the temperature of the petri dish are all the same with 305.15 K. The water shall cool down on its own, caused by the evaporative cooling to check the accuracy of the solver. As shown in Fig. 6, the water should reach a terminal temperature of 300.5 K, which nearly complies with the measured 300.65 K. To calculate this, Star-CCM+ uses an approach in which the phases are in an equilibrium at the interface. Using Raoult's law, this leads to an approximated final evaporation rate for one cell:

$$\dot{M}'_{i,c} \approx -\frac{\rho_g D_{g,i} \nabla Y_{g,m} \nabla \alpha_l V_c}{1 - \sum_{j=1}^{N_v} Y_{g,j}^s}$$

in which ρ is the density, D the diffusion coefficient, α the volume fraction, N the number of components undergoing phase change, V the volume of a cell, and Y the components mass fraction (Siemens, 2019). Depending on the subscript, they denote a gas phase variable (g) or a liquid phase variable (l).

In this context Star-CCM+ does not allow the calibration of the mathematics to match experimental data and is only based on the diffusion of species, which makes the result much more trustworthy. As shown in Fig. 7 the higher humidity around the petri dish and the transportation of the gas phase is visible. Caused by the evaporative cooling the temperature of the water and the petri dish decreases. The simulation was never finished, neither for the water temperature nor for the full evaporation due to the time consuming process. The first 3000 s in Fig. 6 needed 27 days on the presented workstation. This is partly caused by the small time-step, which is necessary to track the water surface and interface properly. To simulate the 36 hours of the experiment, the workstation would need a minimum of 1200 days, which is in this context no appropriate solution.

4.4 PreonLab

The last software is PreonLab as a representative of the

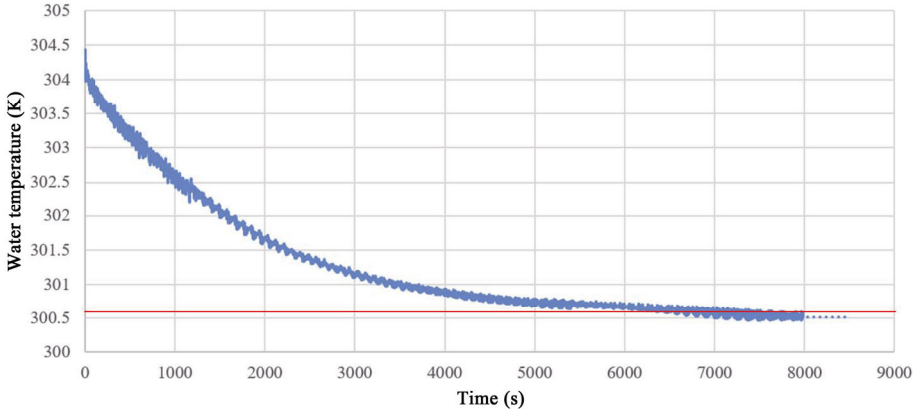

Fig. 6 Result of the simulated water temperature during the evaporation process compared to experimental target value.

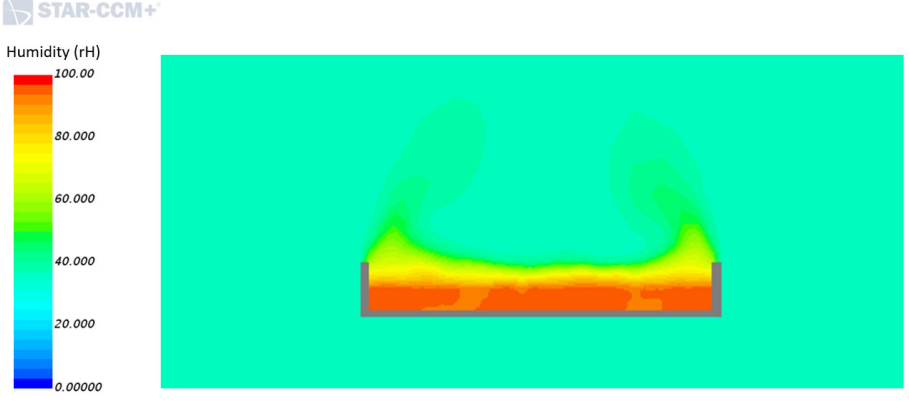

Fig. 7 Distribution of humidity in the room in Star-CCM+.

meshfree SPH-method. PreonLab does not simulate the air directly, because of the high density ratio between water and air. To simulate evaporation, an air box has to be defined with artificial physical conditions, which have to be defined by the user, e.g., temperature, humidity, and wind speed. This leads to a simpler calculation of the mass transportation by approximating the changes in the physical conditions for the whole air box. Evaporated particles are removed from the simulation. Based on this PreonLab computes the evaporation rate with the following equation:

$$m_{\text{evap}} = (coeff + coeff_{\text{wind}} * v_{\text{wind}}) * A * (\tilde{q}_s - \tilde{q})$$

with $coeff_{\text{wind}}$ as a calibration value for the influence of the airflow, $coeff$ as a calibration value for the evaporation based on diffusion and for $\tilde{q}$ the humidity ratio (Fifty2 Technology GmbH, 2019). Because of the low air movement, the influence of the airflow is neglected. The duration of the evaporation can be matched to experimental data due to the calibration value, which also leads to a questionable transferability. To get a better impression of the lowering of the water level the particle size is chosen to represent the amount of water with around 11 layers of particles, which leads to a total particle number of 738,000 (Fig. 8). The simulation of the experimental duration takes around 45 min on the workstation.

Defining a fixed water temperature, the only comparable result in PreonLab is the reduction of the water, since the user defines every other parameter. PreonLab is calibrated to be as close to the 36 h as possible with the last evaporated water particle. As shown in Fig. 9, both graphs show an overall linear course, although PreonLab is wavy at the beginning. PreonLab also shows a delay in the start of the evaporation process. The graph from the simulation can be laid over the graph of the scale and would perfectly end at 31 h.

4 Conclusions

There are as many ways to calculate the evaporation, as there are software solutions on the market. The term of the evaporation does not differentiate between the phase change of a liquid at its saturation point or below in the CFD-tools although it needs a different mathematical calculation and is precisely defined. To define what works best is not generally possible and depends on the applied scenario. The exact calculation of the evaporation is not reliably feasible yet or just for a very small amount or specific scenarios with a short time range. In this context, an often used more artificial approach is the calibratable calculation for the evaporation rate. Based on experimental data, an exact calibration of the simulation model is possible. Using the same model for another scenario is often not feasible or strongly limited. In the end of this analysis are two main statements for evaporation under natural conditions. On the one side is the mesh-based conventional CFD, which is capable of simulating the process correct, but has a massive computation requirement. Even simulating a short experiment in this field of application is not economically realizable. Further optimizations are needed to improve the computation time. On the other side are the meshfree methods, which are much faster but this is the result of numerous assumptions and simplifications. Through the experimental calibration, an application is limited to a few scenarios. Further development with respect to a more detailed air phase

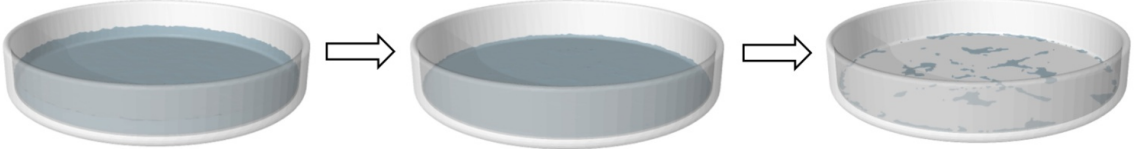

Fig. 8 Process of the water evaporation in PreonLab.

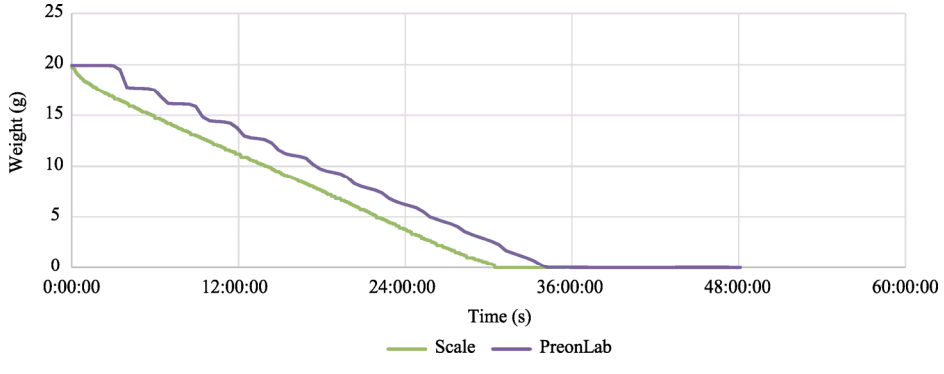

Fig. 9 Comparison of the mass reduction between PreonLab and experimental data.

would be recommended. In search for an exact solution, the best way is an approach with respecting to the thermal processes during the phase change. For the determination of the wetting state of components in a machine an artificial solution, as is used in the SPH-method, is recommended. Even through there will be less accuracy in the calculated result, it is at least possible to calculate a solution in a reasonable amount of time. This solution can be the starting point for appropriate countermeasures for an accelerated drying process of the components.

Acknowledgements

Thanks to the Mercedes-Benz AG for making this research possible by providing financial support.

Funding note

Open access funding provided by Projekt DEAL

References

Alizadehdakhel, A., Rahimi, M., Alsairafi, A. A. 2010. CFD modeling of flow and heat transfer in a thermosyphon. *Int Commun Heat Mass*, 37: 312–318.

ANSYS Inc. 2013. *Ansys Fluent Theory Guide*.

Becker, M., Teschner, M. 2007. Weakly compressible SPH for free surface flows. In: Proceedings of the 2007 ACM SIGGRAPH, DOI: 10.1145/1272690.1272719.

Comsol. 2019. Evaporative cooling of water. Available at: https://www.comsol.de/model/evaporative-cooling-of-water-6192.

Ferziger, J. H., Peric, M. 2008. *Numerische Strömungsmechanik*. Berlin Heidelberg: Springer-Verlag.

Fifty2 Technology GmbH. 2019. *PreonLab 3.2.3 Manual*.

Hermsdorf, F., Jahn, C., Prokop, G. 2016. A multiscale approach to virtually render fluid dynamics on overall vehicle level. In: Proceedingsof the 16. Internationales Stuttgarter Symposium, 287–299.

Hirt, C., Nichols, B. 1981. Volume of fluid (VOF) method for the dynamics of free boundaries. *J Comput Phys*, 39: 201–225.

Ihmsen, M. 2013. *Particle-based Simulation of Large Bodies of Water with Bubbles, Spray and Foam*. Albert-Ludwigs-Universität Freiburg im Breisgau.

Jahn, C., Prokop, G. 2016. Overview and summary of the results of a three-year long term study of corrosion-climatic stresses in an entire vehicle in a real-world use cycle. In: Proceedings of the EUROCORR 2016.

Kraume, M. 2012. *Transportvorgänge in der Verfahrenstechnik*. Berlin Heidelberg: Springer Berlin Heidelberg.

Liu, M. B., Liu, G. R. 2010. Smoothed particle hydrodynamics (SPH): An overview and recent developments. *Arch Comput Method E*, 17: 25–76.

Monaghan, J. J. 1992. Smoothed particle hydrodynamics. *Annu Rev Astron Astr*, 30: 543–574.

Schwarze, R. 2013. *CFD-Modellierung: Grundlagen und Anwendungen bei Strömungsprozessen*, *CFD-Modellierung*. Berlin Heidelberg: Springer Berlin Heidelberg.

Siemens. 2019. *Simcenter STAR-CCM + Documentation*.

Skolaut, W. 2018. *Maschinenbau*. Berlin, Heidelberg: Springer Berlin Heidelberg.

Sun, D. L., Tao, W. Q. 2010. A coupled volume-of-fluid and level set (VOSET) method for computing incompressible two-phase flows. *Int J Heat Mass Tran*, 53: 645–655.

Sun, D., Xu, J., Chen, Q. 2014. Modeling of the evaporation and condensation phase-change problems with FLUENT. *Numer Heat Tr B: Fund*, 66: 326–342.

Sun, X., Sakai, M., Yamada, Y. 2013. Three-dimensional simulation of a solid-liquid flow by the DEM-SPH method. *J Comput Phys*, 248: 147–176.

Wickert, D., Hermsdorf, F., Prokop, G. 2020. Analysis of the water management on a full virtual car using computational fluid dynamics. *SAE Int J Mater Manf*, 13: 05-13-02-0013.